Pure and Applied Geophysics

Three Decades of Seismic Activity at Mt. Vesuvius: 1972–2000

Giuseppe De Natale,[1] Igor Kuznetzov,[2,4] Tatiana Kronrod,[2,4]
Antonella Peresan,[3] Angela Saraò,[3] Claudia Troise,[1]
and Giuliano F. Panza[3,4]

Abstract — We analyse the seismic catalogue of the local earthquakes which occurred at Somma-Vesuvius volcano in the past three decades (1972–2000). The seismicity in this period can be described as composed of a background level, characterised by a low and rather uniform rate of energy release and by sporadic periods of increased seismic activity. Such relatively intense seismicity periods are characterised by energy rates and magnitudes progressively increasing in the critical periods. The analysis of the *b* value in the whole period evidences a well-defined pattern, with values of *b* progressively decreasing, from about 1.8 at the beginning of the considered period, to about 1.0 at present. This steady variation indicates an increasing dynamics in the volcanic system. Within this general trend it is possible to identify a substructure in the time sequence of the seismic events, formed by the alternating episodes of quiescence and activity. The analysis of the source moment tensor of the largest earthquakes shows that the processes at the seismic source are generally not consistent with simple double-couples, but that they are compatible with isotropic components, mostly indicating volumetric expansion. These components are shown to be statistically significant for most of the analysed events. Such focal mechanisms can be interpreted as the effect of explosion phenomena, possibly related to volatile exsolution from the crystallising magma.

The availability of a reduced amount of high quality data necessary for the inversion of the source moment tensor, the still limited period of systematic observation of Vesuvius micro-earthquakes and, above all, the absence of eruptive events during such interval of time, cannot obviously permit the outlining of any formal premonitory signal. Nevertheless, the analysis reported in this paper indicates a progressively evolving dynamics, characterised by a generally increasing trend in the seismic activity in the volcanic system and by a significant volumetric component of recent major events, thus posing serious concern for a future evolution towards eruptive activity.

Key words: Seismicity, microearthquakes, earthquake-source mechanism, earthquake catalogue, *b* values, Vesuvius.

[1] Osservatorio Vesuviano, Napoli, Italy.

[2] Russian Academy of Sciences. International Institute of Earthquake Prediction Theory and Mathematical Geophysics, Moscow, Russian Federation.

[3] Department of Earth Sciences, University of Trieste, Trieste, Italy.
E-mail: anto@dst.units.it

[4] The Abdus Salam International Centre for Theoretical Physics – ICTP, Miramare, Trieste, Italy.

Introduction

Somma-Vesuvius is probably the most famous volcano in the world, mainly due to its large plinian eruption in Roman times (79 A.D.), which completely buried the towns of Herculaneum and Pompeii under several meters of pyroclastic and mud flows. Today, the risk of eruptions at Somma-Vesuvius is the highest in the world, because more than 700,000 people live within a radius of 10 km from the crater, an area with the maximum hazard for pyroclastic flows from plinian and subplinian eruptions. The eruptive activity of this volcano appears composed of main cycles, which start with plinian or subplinian eruptions and, after centuries of mainly effusive to moderate explosive activity, terminate with an eruption which closes the conduit (no magma in the crater anymore) (SANTACROCE, 1987). The last eruptive cycle started in 1631, with a violent subplinian eruption (ROLANDI *et al.*, 1993; ROSI *et al.*, 1993; SCANDONE *et al.*, 1993), and ended in 1944, when the last, modest, eruption closed the main conduits. According to several observations and volcano-logical models (SANTACROCE, 1987) the next eruption, which should open a new eruptive cycle, has a considerable probability of being a subplinian or plinian one. The very strong concern for a future eruption of this kind compelled the Italian government to prepare an evacuation plan of the whole area, in case the scientific monitoring network should record signals of an impending eruption. The careful analysis of geophysical data at this area is then of extreme importance, both for the high scientific interest of the area, and for the extreme risk involved. The main obstacle for the forecast of a future eruption in this area is the preponderant lack of knowledge regarding the precise dynamics before violently explosive eruptions. We historically reference the Roman and Spanish chronicles of the 79 and 1631 eruptions (ROSI *et al.*, 1993), but they are obviously not very useful for comparisons with the outputs from modern monitoring techniques. Several historical studies point out the lack of very high magnitude earthquakes before the eruptions (SIGURDSSON *et al.*, 1985; ROSI *et al.*, 1993), with the possible exception of an event which occurred in 62 A.D. 17 years before the 79 eruption (MARTURANO and RINALDIS, 1995). It is, however, not yet clear if such an event was really a Vesuvius event, or rather one which occurred in the neighbouring tectonic areas of the Apennine chain.

For all these reasons it is very important to study the seismic catalogue, including also relatively low magnitude events, since the expected magnitudes before eruptions will probably not exceed $M_d = 4$, i.e., they will be of the same size as those recorded in recent years. Despite the importance of the study and interpretation of seismicity in this area, it is only in recent years that various papers have been devoted to the modelling of the seismicity of the Vesuvian area (VILARDO, 1996; CAPUANO *et al.*, 1999; IANNACCONE *et al.*, 2001; MARZOCCHI *et al.*, 2001; VILARDO *et al.*, 2002). Recently, DE NATALE *et al.* (2000) presented a model to explain the mechanisms of the background seismic activity at central volcanoes, with particular reference to Somma-Vesuvius. BERRINO *et al.* (1993) reported the last integrated analysis of geophysical data collected in this area in

20 years of seismic and geodetic monitoring. Recent research on Somma-Vesuvius has been particularly devoted to the determination of the internal structure, in the framework of the large TOMOVES project (ZOLLO et al., 1996; DE NATALE et al., 1998). A close spatial relationship between the internal structure and seismic activity has been evidenced and interpreted by DE NATALE et al. (2000).

In this paper, we compute the focal mechanisms of the largest events ($M_d > 3.0$), using a method based on the computation of the full moment tensor of the events (SILENY et al., 1992; SILENY, 1998) and we analyse the seismic catalogue of the last three decades of seismic activity at Somma-Vesuvius. The catalogue is based on the recordings at the station OVO, located at the Osservatorio Vesuviano building on Vesuvius, which was installed in 1972 and is equipped, since that time, with a three component Geotech S-13 sensor. We perform the analysis of energy release, as well as of the b value as a function of time, and we evidence a substructure in the seismicity, consisting of alternating periods of quiescence and activity that point out an increasing trend of the local seismic activity.

The Seismic Catalogue

The seismic catalogue of Vesuvius microearthquakes, hereinafter referred to as OV2, consists of a revised list of about 9000 local earthquakes recorded since 1972 at the station OVO (Fig. 1). The station, located at the site of the ancient building of Osservatorio Vesuviano, is equipped with 3 Geotech S-13 geophones, oriented along the three principal directions (N, E, V). The OVO station represents the first modern seismometer installed on the Vesuvius volcanic edifice, and the instrumentation has been unchanged since then, therefore it provides the longest homogeneous catalogue of the events which occurred at Vesuvius.

The magnitude of the events is determined from the time duration, according to DEL PEZZO et al. (1983), who compared recordings of aftershocks of the 1980 $M_L = 6.9$ Irpinia earthquake at the station OVO with the local magnitudes computed for the same events at the station located at Monte Mario, near Rome (National Institute of Geophysics), equipped at that time with a Wood-Anderson instrument. The magnitudes estimated for the events recorded at the OVO station range from slightly less than 0 to 3.6.

The stations equipment remained unchanged since its installation and the same magnitude type, M_d, is reported for all the events, therefore the precision of magnitudes determination is expected to be uniform in time. This allows us to consider the entire period of observations to perform the analysis of "magnitude grouping", which enables to evidentiate as to whether there are dominating values of magnitudes, due for example to a different accuracy of the amplitude measurements for events in different magnitude ranges. Such preliminary analysis is useful to choose the appropriate intervals of magnitude grouping to be considered for the frequency-
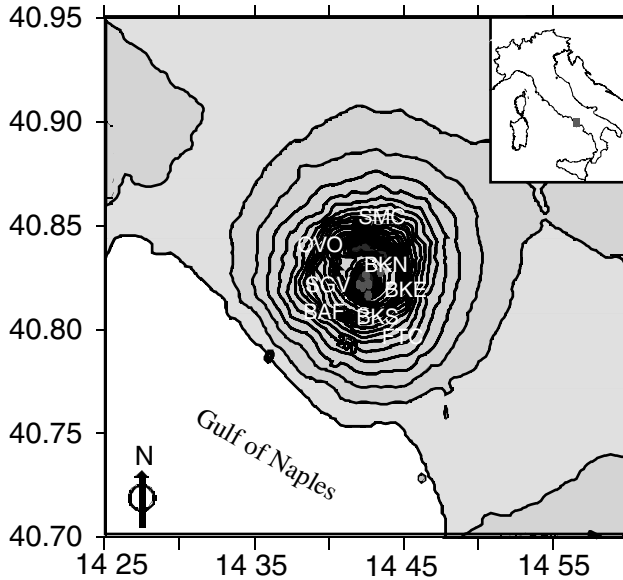
Figure 1
Somma-Vesuvius area, with contour lines and the location of the recording stations whose data have been employed in this study.

magnitude distribution; hence it is necessary both for the analysis of the catalogue completeness and for the estimation of the parameters of the frequency-magnitude relation (FMR). The distribution of the percentage of events versus magnitude is considered, with a very small magnitude step ($\Delta M = 0.1$), for three subsequent magnitude intervals: [0.4; 1.3], [1.4; 2.3] and [2.4; 3.3], as shown in Figures 2a, 2b and 2c respectively. It is possible to observe from Figure 2 that the weaker are the events, the more clear appears the magnitude grouping, i.e., some values of the decimal digit of M are more frequent than others and there are some gaps in the distribution. Thus, in the magnitude range $0.6 \leq M \leq 1.4$ the values 0.6, 0.9 and 1.2 appear dominant (Figs. 2a and 2b), i.e., the magnitude is grouped with the step $\Delta M = 0.3$. Similarly, for $1.5 \leq M \leq 2.1$ the grouping step is $\Delta M = 0.2$ (values 1.5, 1.7, 1.9 are predominant, while there are gaps for 1.6, 1.8 and 2.0). The largest events, with $M \geq 2.2$, are not really grouped, i.e., they are grouped uniformly with the step $\Delta M = 0.1$ which is conditioned by the assumed format of the magnitude presentation. This analysis, repeated considering different time windows (figures are not reported), confirms that the evidenced magnitude grouping does not change in time.

The completeness of the catalogue can then be visually determined from the frequency-magnitude distribution, that is considering the distribution $\lambda(M)$ of the number of earthquakes within each magnitude grouping interval ΔM. Figure 3 shows the differential and cumulative graphs of $\log \lambda(M)$ for each of the three decades of seismic activity, normalised to the space-time-magnitude volume unit
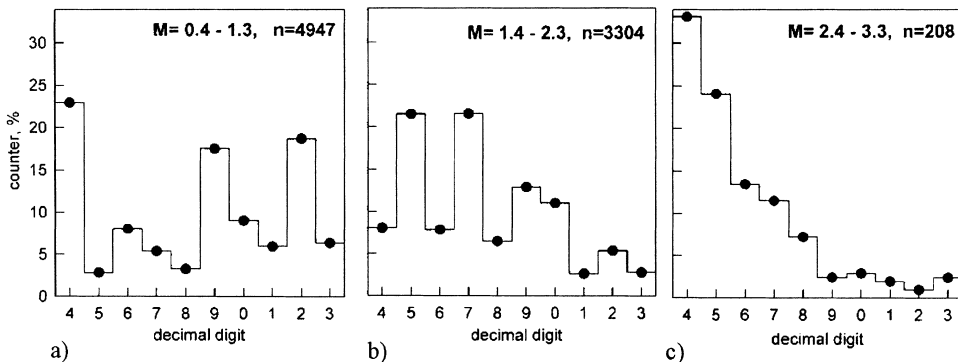
Figure 2
Distribution of the number (percentage) of events versus magnitude (decimal digit) for three adjacent magnitude intervals, considering all the events reported in the OV2 catalogue.
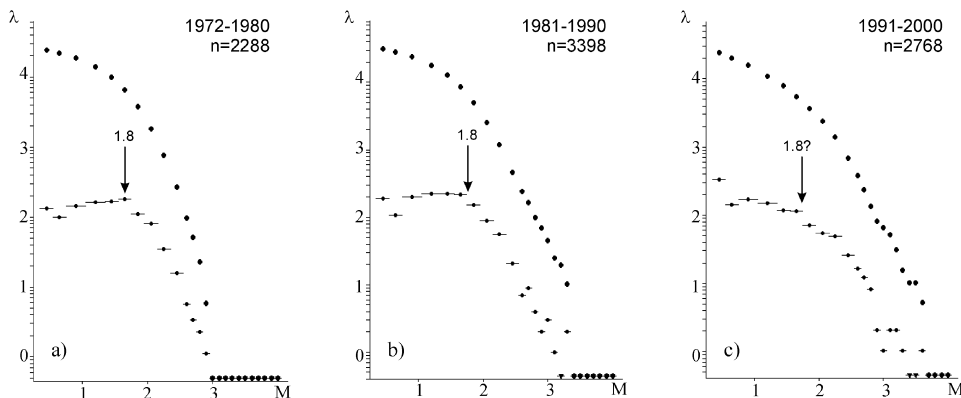

Figure 3
Differential (dots with horizontal bars) and cumulative graphs (dots) of log $\lambda(M)$ for three subsequent time periods, where λ is the number of earthquakes per space-time-magnitude volume unit $V = [1000 \text{ km}^2 \times 1 \text{ year} \times 1 \text{ M}]$. The amplitude of the magnitude grouping intervals ΔM is given by the horizontal segments, while the solid circles at their centres indicate the value of λ. The arrows indicate the selected magnitude cut-off.

$V = [1000 \text{ km}^2 \times 1 \text{ M} \times 1 \text{ year}]$. The cut-off M_{min} is fixed corresponding to the magnitude below which the empirical graph log $\lambda(M)$ deviates from linearity. This set of graphs shows that the deviation from linearity appears more clearly from the non-cumulative distribution than from the cumulative one. The differential graphs log $\lambda(M)$ shown in Figures 3a and 3b indicate that the completeness magnitude cut-off can be confidently fixed at $M_{min} = 1.8$. The distribution shown in Figure 3c appears rather different: a smooth, continuous deviation from linearity is obtained instead of the abrupt change, even in the differential distribution. This difference might be related to the incomplete observations of the weaker events on the background of the stronger events (it is in this period that the strongest earthquake,

with $M = 3.6$, occurred), but it might also result from a change in the seismic regime. Though the magnitude threshold for the completeness of the catalogue appears to be even lower during some limited intervals of time, we have established to keep $M_{min} = 1.8$ for the entire period of observation and not to use a variable $M_{min}(T)$, since we know very little about the stability of FMR at such small magnitudes. The completeness threshold $M_d = 1.8$ appears rather high for such small volcanic earthquakes; this high threshold is mainly caused by the high noise due to the urbanisation of the area.

Analysis of Seismicity

A reliable analysis of the time features of seismicity requires to consider of only the complete part of the catalogue, thus eliminating the smallest events, which are not systematically recorded. The time sequence and the yearly distribution (considering non-overlapping time windows) of the events with $M \geq 1.8$, recorded at the OVO station in the period 1972–2000, is then considered as shown in Figure 4. It is clear, from this figure, that a background seismicity is always present at Somma-Vesuvius, with a minimum rate of some tens of earthquakes per month, while periods of increased seismic activity, both in number and in magnitude of the events, can be
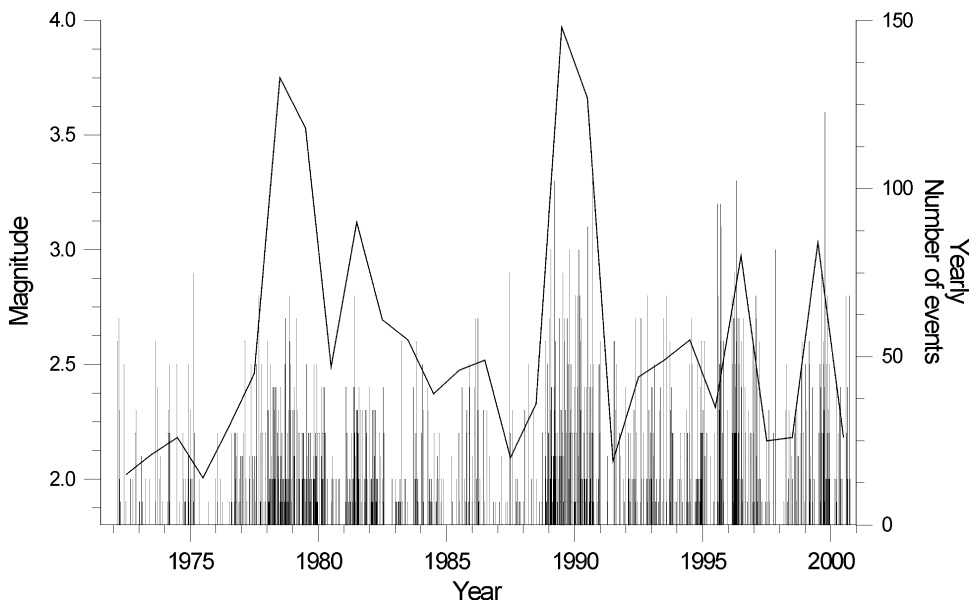

Figure 4
Time sequence of the events $M(t)$ and yearly number of earthquakes (non-overlapping time windows) with $M \geq M_{min} = 1.8$ reported in the OV2 catalogue, from 1972 to 2000.

evidenced in these time sequences. A high number of earthquakes, however, is not necessarily associated with high magnitudes; for example, the seismic swarm in the period 1978–1980 is characterised only by moderate events ($M < 3.0$), while the largest earthquake ($M_d = 3.6$), which occurred in October 1999, is accompanied by a relatively small number of events with $M \geq M_{\min} = 1.8$.

The seismic energy release is then studied considering the quantity E^*, computed from magnitude according to the formula:

$$E^* = 10^{d(M-M_{\min})} \quad d = \text{const.} \tag{1}$$

E^* represents the energy release normalised to the energy of the minimum magnitude event considered in the analysis, that is $M_{\min} = M_{\text{completeness}} = 1.8$:

$$E^* = \frac{E}{E_{\min}} = \frac{10^{c+dM}}{10^{c+dM_{\min}}} \quad c, d = \text{const.} \tag{2}$$

The considered relationship between the energy E and the magnitude M has the classical form proposed by GUTENBERG and RICHTER (1956). The use of the normalised energy E^* allows us to make the analysis less sensitive to the choice of the empirical parameters c and d of the energy-magnitude relation, since only the coefficient d is required. In this study, to be conservative in outlining the trend of the energy release rate, we use the value $d = 1.5$, given by GUTENBERG and RICHTER (1956) for M_s, even if larger values ($d \approx 2 - 3$) are consistent with M_L (KANAMORI et al.,1993) or M_d (PANZA and PROZOROV, 1991) estimates.

Figure 5 shows the curve of the monthly energy release $E^*(t)$ as a function of time. The energy release exhibits a mostly constant background rate ($E^*_{\text{monthly}} \leq 50$ during about 90% of the period of observation), with sporadic periods of strongly increased rates. The periods of increased energy release are approximately: 1978–1980, 1989–1990, 1995–1996 and 1999–2000. Such anomalous time intervals are characterised (except the first one) by the occurrence of the largest magnitude events. The maximum magnitude and the average energy rate progressively increase with time, while the time intervals between subsequent periods of intense seismicity seem to decrease.

An important step towards the understanding of the time evolution of seismicity can be made by computing the time dependence of the b value in the Gutenberg-Richter (GR) relation (GUTENBERG and RICHTER, 1944; 1956). The rough estimation of the variation in time of the b value in the GR law has been performed, in moving windows containing 100 earthquakes each, shifted by 10 events, using the maximum likelihood method (WIEMER and ZUNIGA, 1994). Until 1986 b smoothly oscillates around the value 1.8; from 1988 to 1996, b is around 1.3; finally since 1996 the b value further decreases to about 1.0 (Fig. 6). The periods of most rapid change in the b value are almost the same periods in which increased energy rate and maximum magnitudes are observed.
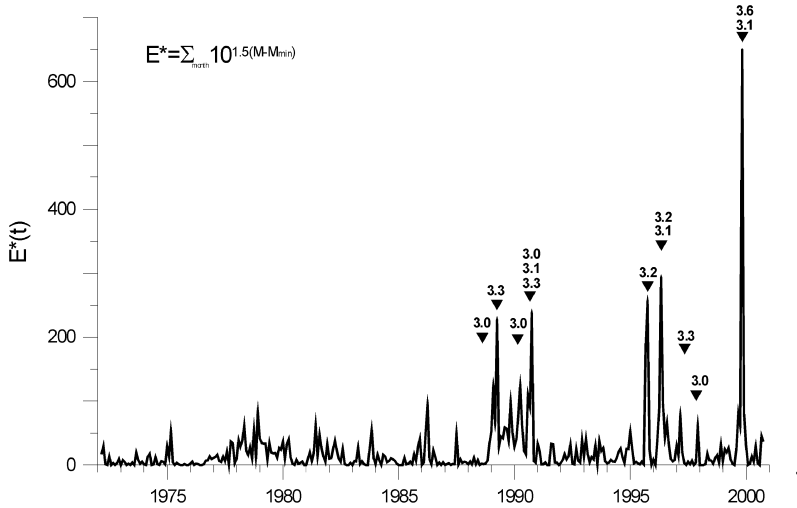
Figure 5

Diagram of the normalized monthly energy release $E^*(t)$ at Somma-Vesuvius, estimated from local earthquake magnitudes, using time windows of one month shifted by one month. Maximum magnitude event's occurrence is indicated by arrows.
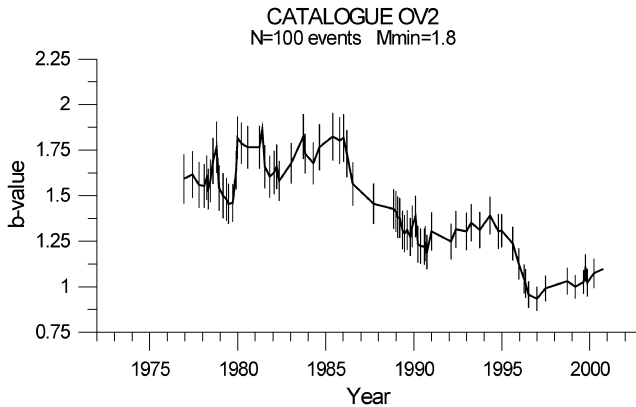

Figure 6

Time variation of the b value, estimated using the maximum likelihood method (WIEMER and ZUNIGA, 1994) considering groups of 100 events, shifted by 10 events; the vertical bars indicate the errors.

For the complete catalogue, we attempt to define in a unequivocally formal way the periods of "quiescence", q, characterised by some typical background seismicity, and the periods of "activity", a, where the energy release is unusually large. With this purpose we compute $E^*(t)$, grouping the events into time windows of one year, shifted by one month, and we consider the distribution of the estimated yearly energy $E^*_{yearly}(t)$, both in the cumulative and discrete form (Fig. 7). From Figure 7 we can
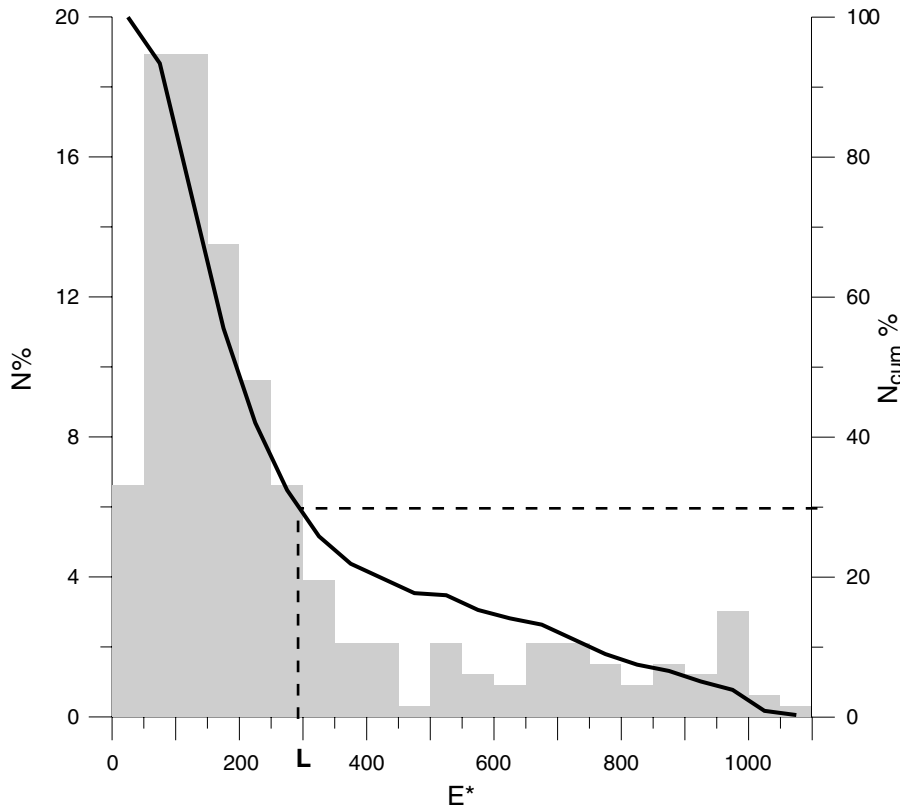
Figure 7
Distribution of the yearly energy release $E^*(t)$, estimated for $M \geq 1.8$ using time windows of one year, shifted by one month. The histogram shows the discrete distribution, the bold line, and the cumulative one. The dotted line indicates the selected threshold $L = 300$, corresponding to 30% of the time intervals.

observe that during most of the time the energy release is contained within a relatively narrow range $50 \leq E^* \leq 300$, and that the energy distribution exhibits a tail extending to quite high values of E^*. Therefore we choose the threshold $L = E^* = 300$, which selects about 30% of the considered time, practically, i.e., during 30% of the period of observation $E^*(t) \geq L = 300$ (see the cumulative distribution in Fig. 7).

The periods of activity are then defined as the time intervals within which the normalised energy release $E^*(t)$ exceeds the threshold L; in Figure 8a the intervals of quiescence and activity are indicated with q1, q2, q3, q4, q5 and a1, a2, a3, a4, respectively (Table 1).

For all the periods identified, as well as for some groups of them, the parameters a and b of the GR law are computed using the maximum likelihood method proposed by MOLCHAN and PODGAETSKAYA (1973), and described in detail in MOLCHAN et al.
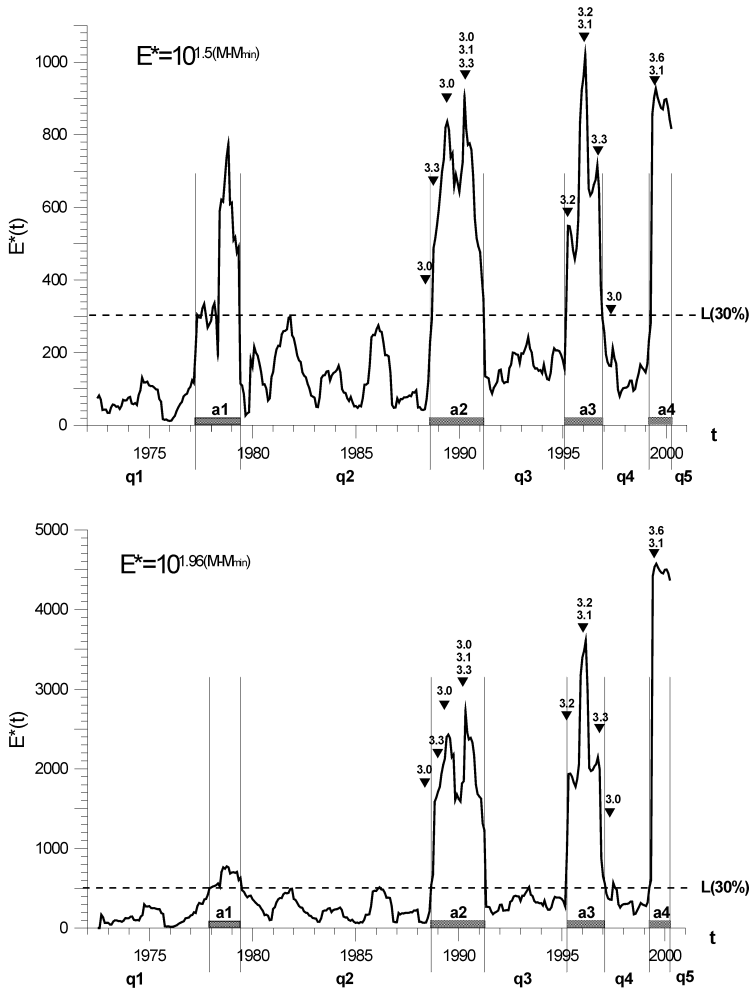
Figure 8

a) $E^*(t)$ determined for events with $M \geq 1.8$ using time windows of one year, shifted by one month, and with $d = 1.5$ (GUTENBERG and RICHTER, 1956). The triangles point to the occurrence of strong events. The grey boxes evidence the periods of activity above the threshold L (a1, a2, a3 and a4), which is indicated by the dotted line. b) The same as Figure 8a, but with $E^*(t)$ estimated considering $d = 1.96$ (KANAMORI *et al.*, 1993).

(1997). A confidence level of 95% is considered for the parameter b, and of 99% for the parameter a, assuming as minimum magnitude cut-off $M_d = 1.8$. The results, summarised in Table 2, confirm in a quantitative way the general trend shown in Figure 6.

The parameters of the GR law obtained for the different time intervals are then compared, both considering individual intervals and composite intervals, the latter being obtained merging the individual samples. The results of the

Table 1

Time intervals (initial and final time) and point estimates of the parameters a,b of the GR law for the different intervals of quiescence and activity, as shown in Figure 8a. N is the number of events within each time window

Interval	Time window	b value		N
		a-intervals	q-intervals	
q1	1972.2.23–1977.10.31		1.59	143
a1	1977.11.1–1979.5.31	1.56		190
q2	1979.6.1–1988.7.31		1.72	482
a2	1988.8.1–1991.2.28	1.32		307
q3	1991.3.2–1995.1.31		1.29	167
a3	1995.2.1–1996.12.1	0.90		107
q4	1996.12.2–1999.2.28		1.08	62
a4	1999.3.1–2000.4.1	1.04		83
q5	2000.4.2–2000.10.9		1.05	21

Table 2

Estimates of the parameters a,b of the GR law for the individual and composite time intervals. N is the number of events within each time window. [b_{min}, b_{max}] indicates the 95% confidence level interval for the parameter b. The value of a is normalised for a time interval of one year, for an area of 1000 km^2 and for a reference magnitude $M_0 = 2$ (MOLCHAN et al., 1997)

Interval	N	$P_b = 95\%$			P_a 99%	
		b	b_{min}	b_{max}	a	Δa
a1	190	1.56	1.34	1.80	2.24	0.165
a2	307	1.32	1.17	1.47	2.22	0.129
a3	107	0.90	0.72	1.11	1.86	0.221
a4	83	1.04	0.81	1.30	2.00	0.251
q1	143	1.59	1.33	1.88	1.56	0.190
q2	482	1.72	1.56	1.88	1.87	0.103
q3	167	1.29	1.09	1.50	1.78	0.176
q4	62	1.08	0.80	1.38	1.56	0.292
q5	21	1.05	0.60	1.59	1.72	0.512
a1 + a2	497	1.40	1.28	1.53	2.32	0.101
a3 + a4	190	0.96	0.81	1.12	1.92	0.165
q1 + q2	625	1.69	1.55	1.83	1.79	0.090
q3 + q4 + q5	250	1.21	1.05	1.37	1.71	0.143
(a1 + a2) + (q1 + q2)	1122	1.53	1.45	1.64	1.93	0.067
(a3 + a4) + (q3 + q4 + q5)	440	1.09	0.98	1.20	1.79	0.108

comparison of the *b* value for individual intervals are presented in Table 3, while the results of the comparison of the parameters *a*, *b* for composite groups of data are shown in Table 4.

The choice of the threshold *L* is rather arbitrary, however several tests made changing the threshold within reasonable intervals, show that the definition of

Table 3

Comparison of the parameter b of the GR law for the different intervals identified in Figure 8a. Nf is the number of degrees of freedom. The b values differ with a significance level of 95%, if the probability π is larger than 95%

Intervals compared	Test/Nf	π %	Conclusion of the comparison
a1, a2, a3, a4	21.8/3	>99.95	*b* values are different
a1, a2	3.1/1	92.6%	the difference in *b* values is not significant
a3, a4	0.7/1	61.0%	the difference in *b* values is not significant
q1, q2, q3, q4, q5	21.5/4	>99.95	*b* values are different
q1, q2	0.6/1	55.0%	the difference in *b* values is not significant
q3, q4, q5	1.7/2	58%	the difference in *b* values is not significant

Table 4

Comparison of the parameters a,b of the GR law for the different composite time intervals of activity and quiescence. Nf is the number of degrees of freedom. The b values differ with a significance level of 95%, if the probability π is larger than 95%

Composite samples	N	b	b_{min}	b_{max}	a	Δa	Test/Nf*	π %	Conclusion
a1 + a2	497	1.37	1.26	1.49	2.20	.095	17.91/1	>99.95	*b* values are different
a3 + a4	190	0.96	0.81	1.12	1.92	.165			
q1 + q2	625	1.69	1.55	1.84	1.77	.096	19.17/1	>99.95	*b* values are different
q3 + q4 + q5	250	1.21	1.05	1.37	1.71	.143			
a1 + a2 + q1 + q2	1122	1.51	1.42	1.61	1.93	.067	36.69/1	>99.95	*b* values are different
a3 + a4 + q3 + q4 + q5	440	1.09	.98	1.20	1.79	.108			

quiescence and activity periods varies only moderately, and consequently the values of *a* and *b* are quite stable.

Finally, in order to verify the stability of the results with respect to the choice of the coefficient *d* in the equation (1), the analysis has been repeated considering a different energy-magnitude relation. We consider, for example, the value $d = 1.96$ proposed by KANAMORI *et al.* (1993) to compute the quantity $E^*(t)$ and the corresponding threshold *L* (Fig. 8b). Comparing Figures 8a and 8b, it is possible to observe that the time intervals of activity and quiescence thus identified do not differ significantly, the main variation being a larger increasing trend of the energy release rate in Figure 8b.

The seismicity does not appear as a periodic expression of a repetitive underlying process, rather it seems to evolve with periods of intense activity (1989; 1995–1996; 1999). The decrement of the *b* value (Fig. 6) indicates the increase with increasing time of the rate of the large events, in agreement with the progressive growth, from 1988 to 1999, of the maximum observed magnitude (from 3.2 to 3.6). The first

decrease of b occurs just before the crisis of 1989. The parameters estimated for the intervals of quiescence and activity (Tables 1 and 2), confirm the general decrement of the b value with increasing time. The two GR laws obtained for the time periods [a1 + a2 + q1 + q2] ($b = 1.51 \pm 0.09$) and [a3 + a4 + q3 + q4 + q5] ($b = 1.09 \pm 0.11$), that is before and after February 1991, differ with a confidence level of 99.95%.

Earthquake Source Processes

We study the earthquake sources of the largest events with two different approaches. The first (method 1), originally developed by BRUNE (1970), permits the estimation of the scalar seismic moment M_0 from the amplitude, at low frequency, of the displacement spectra in the assumption that the source mechanism can be satisfactorily represented by a double-couple; the second (method 2), based on the waveform inversion, retrieves the full seismic moment tensor without any *a priori* constraints on the source mechanism. Indeed the seismic moment tensor can be decomposed into double-couple (DC), compensated linear vector dipole (CLVD) and volumetric (V) components, and it is very suitable to investigate the physical changes within a volcano, related to magma or fluid movements (e.g., KNOPOFF and RANDALL, 1970; JOST and HERRMANN, 1989).

To determine the full seismic moment tensor we apply the method developed by SILENY *et al.* (1992), SILENY (1998). The method, already applied in volcanic areas (e.g., CAMPUS *et al.*, 1993; SARAÒ *et al.*, 2001), works in the point source approximation and consists of two main steps: 1) unconstrained linear inversion to retrieve, from the recorded seismograms, the six moment rate functions (MTRF) and 2) constrained nonlinear inversion where the MTRF's are used as data to obtain the focal mechanism, the scalar seismic moment and the source time function. In the *first step* the moment rate functions are obtained by deconvolution of the Green's functions from the data. The synthetic Green's functions are computed by modal-summation technique (e.g., PANZA, 1985; FLORSCH *et al.*, 1991; PANZA *et al.*, 2001) for a grid defined by a range of hypocentral coordinates and by two structural models assumed to be representative of the model space around the source and the recording station. At a generic point within the space where the grid is defined, the Green's function is determined by interpolating the Green's functions computed, for the two structural models, at nearby grid points. Once the Green's functions are determined, the MTRFs are obtained applying a method based on SIPKIN (1982) approach to obtain reliable moment rate functions when processing local high-frequency waveforms, and by using a parameterisation of the moment rate functions by a series of triangles overlapping in their half-width (NABELEK, 1984). With the retrieved MTRFs, synthetic seismograms are computed and compared with the observed ones. The L_2 norm of their residuals is minimized by an iterative process

that singles out the minimum corresponding to the best MTRFs which can be considered as solution of the first step.

In the second step, assuming that for a weak event it is reasonable to expect a constant mechanism during the energy release, we search for their correlated part. The problem is nonlinear and it is solved iteratively by imposing constraints such as positivity of the source time function and the requirement that the equal polarity areas are distributed consistently with clear readings of first arrival polarities, when these are available. The mechanism and the source time function are obtained after factorization of the MTRFs. The factorization of the MTRFs reduces the bias due to the modelling of the Green's function since it works only on their coherent part. The predicted MTRFs are then matched to the observed MTRFs obtained as output of the first step.

The advantage of this approach is a simplification of the problem of fitting the input seismograms by converting it into a problem of matching the MTRFs. The number of MTRFs is fixed at six, or five when dealing with only deviatoric sources, and their length is controlled by the number of triangles used for their parameterization. Considering the MTRFs as an independent function in step 1 leads to an overparameterization of the problem which is advantageous to absorb inadequate modeling of the structure (KRAVANJA *et al.*, 1999). The effects due to local heterogeneities and to wave propagation, such as attenuation, reflection or scattering, are in this way reduced. The effects of inadequacies of the structural models have been investigated by SILENY *et al.* (1992), KRAVANJA *et al.* (1999). Starting from a double-couple mechanism with an instantaneous source time function they proved, by synthetic tests, that a poorly known structure, not contained in the allowed interpolation range of the Green's functions (1) causes mainly the presence of apparent non-double-couple components in the moment tensor solutions and contaminates particularly the CLVD that increases from 0% of the starting model to 40% for large inconsistency cases; (2) does not affect the orientation of the double-couple that remains stable within $\pm 10°$, and (3) leads to spurious peaks in the source time function (KRAVANJA *et al.*, 1999). Mislocation of the hypocentre and the use of an inadequate model of the medium may enlarge the error bars of the source time function by about 20%. Nevertheless, when introducing the variance due to the noise present in the data and to the modelling of the Green's functions, the error analysis (SILENY *et al.*, 1996; SILENY, 1998) indicates the level of reliability of the solutions (PANZA and SARAÒ, 2000). On the other hand if the percentage of non-double-couple components can be affected by systematic errors due to poor structural modeling, when looking at data sharing similar paths in the same area, their variation and the observed trend are free from such a shortcoming (SARAÒ *et al.*, 2001).

Tests done on synthetic data have also shown that the inversion results are stable until the noise in the data is less than 20% of the maximum amplitude (SILENY *et al.*, 1996; CESPUGLIO *et al.*, 1996). The solutions are stable even when few stations are used (SILENY *et al.*, 1992). Indeed for the determination of the six independent

components of the moment tensor in time domain, the six independent data are obtained from P, SV and SH arrivals at two stations (e.g., STUMP and JOHNSON, 1977; PANZA and SARAÒ, 2000) and two three-component stations or three vertical component stations, are mathematically sufficient, to solve the moment tensor components.

Data Analysis and Results

From the seismicity which occurred at Mt. Vesuvius during the period 1989–1997 we studied six events, located in the central part of the volcano, with duration magnitude greater or equal to 3.0 (Table 5) for which digital waveforms were available. Noisy seismograms, or data for which the epicentral distance was too small compared with the hypocentral depth computed by standard routine (HYPO71) are not included. The latter condition is necessary for a straightforward application of the modal-summation technique when computing the Green's function. A minimum of four signals, depending on the quality of the data, is required for each inversion. The recording stations (Fig. 1) are run by Osservatorio Vesuviano and are equipped with geophones Mark L4-3-D with natural period of 1 s. The velocities, recorded at a sampling frequency of 125 Hz, have been resampled at 20 Hz. On the basis of several tests to guarantee clear arrivals and high signal-noise ratios, as a rule, we low-pass filter seismograms at 5 Hz using a gaussian filter. After mean removing, tapering and filtering, we select the temporal window of the seismograms to be inverted.

For the waveform inversion the Green's functions are computed employing different structural models for each path source-station and for the source area that practically coincides with the center of the volcano. Each structure is adjusted from the 3-D velocity model proposed by DE NATALE et al. (1998) and from the attenuation values reported in BIANCO et al. (1999). The density values are computed using the empirical Nafe-Drake curves.

Table 5

The focal depth is referred to 0.9 km above the sea level. M_0 is the scalar seismic moment computed by Brune approach (method 1) and by moment tensor analysis (method 2)

N.	Date	Focal depth (km)	M_d	Method 1 $M_0 \times 10^{13}$ Nm	Method 2 $M_0 \times 10^{13}$ Nm
1	19.3.1989	1.6	3.3	5.8 ± 3.1	1.4 ± 0.6
2	24.9.1995	2.4	3.1	3.1 ± 0.6	1.4 ± 0.4
3	25.4.1996	3.5	3.3	2.4 ± 0.7	4.8 ± 0.3
4	5.11.1997	3.2	3.0	2.0 ± 1.0	1.0 ± 0.3
5	9.10.1999	3.9	3.6	11.1 ± 5.0	6.6 ± 1.1
6	11.10.1999	2.8	3.1	1.9 ± 0.8	2.2 ± 0.1

To reduce the number of unknowns and to make more stable the results of the inversions, we fix the epicentre—the best constrained parameter by routine locations—of the studied events to the values computed by OV and we invert only for the hypocentral depth and the six components of the moment tensor. The damping value used in the inversion has been selected, after several tests, equal to 10^{-2} to minimize the spurious non-DC components.

Whenever possible, inversions for the same event considering either different sets of records or introducing a kinematical correction for the station elevation have been performed to test the stability of the results. Moreover since spurious non-double couple components can arise only resulting from the station configuration (PANZA and SARAÒ, 2000), we performed synthetic tests to define lower limits above which the non-double couple components found can be considered statistically significant. The main results obtained for the six studied earthquakes are reported in Table 5.

In Figure 9 the results of the waveform inversion are given. The fit of the data against synthetic signals is reported for all the studied events. The common feature to most of the studied events is the existence of a relevant V component (Fig. 10) that is consistent with the presence of magmatic degassing processes and of superheating of the water-bearing stratum. The presence of a V component in the 1996, April 25 event, was estimated by the independent analysis of VILARDO (1996).

The comparison with the Etna seismicity studied by SARAÒ *et al.* (2001) shows that the V component is more relevant for the Vesuvius events.

Discussion and Conclusions

DE NATALE *et al.* (2000) showed that the local seismicity at Somma-Vesuvius is strongly clustered around the crater axis, i.e., within less than 1 km from the crater centre, in the depth range 0–6 km. A certain level of background activity is always present at this volcano. Despite the overall constancy of the seismically active volume, we have shown that time and energy distribution of the events does not appear constant in the last three decades. DE NATALE *et al.* (2000) interpreted the seismic background mainly in terms of local gravitative loading of the volcanic edifice, focused around the crater axis by a marked rigidity anomaly. The accurate analyses of the seismic catalogue presented in this paper, however, show that seismicity cannot be entirely considered as a simple background activity with constant properties. In fact, it consists of periods of alternating low and high seismicity levels. The curve of the monthly energy release, computed along the three decades spanned by the catalogue, shows clearly that the low seismicity levels are characterised by an energy rate with features rather uniform in time. Such a rate of energy release during low activity periods can be considered representative of the background seismic level. Superimposed to such background activity, intense seismicity episodes occasionally occur. Differently from those of low seismicity,
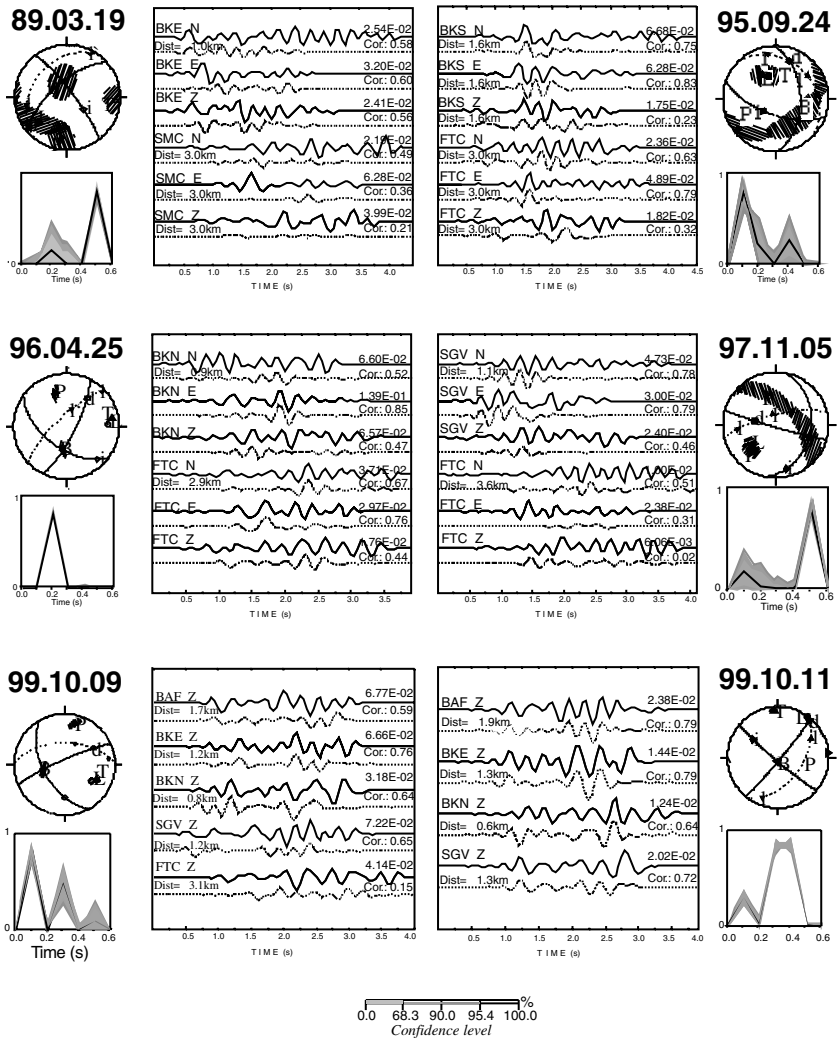
Figure 9

Results from the waveform inversion of the events listed in Table 5. — Real data (solid line) and synthetic signals (dotted line): the epicentral distances, the station name and the component used are reported on the left of the panel, whereas the maximum amplitudes and the correlation values are reported on the right. — Focal mechanism with confidence error ellipses in the RIEDESEL-JORDAN (1989) representation: *L* is the vector describing the total mechanism, *d* is the *DC* vector, *l* and *l′* are the CLVD with major dipole along the tensional and the pressure axes respectively, *i* represents *V*. *T*, *P* and *B* indicate the tensional, compression and null axes respectively. The dashed line represents the locus of the deviatoric mechanism. Hatched areas around the *L*, *P*, *T*, *B* axes are the projections of the 97% confidence ellipses onto the focal sphere. The distance of *L* from the vectors *i*, *d*, *l*, and *l′* displays the share of *V*, *DC* and CLVD part that can be considered reliable. – Source time function: the error bars are plotted with a grey scale according to different values of confidence.
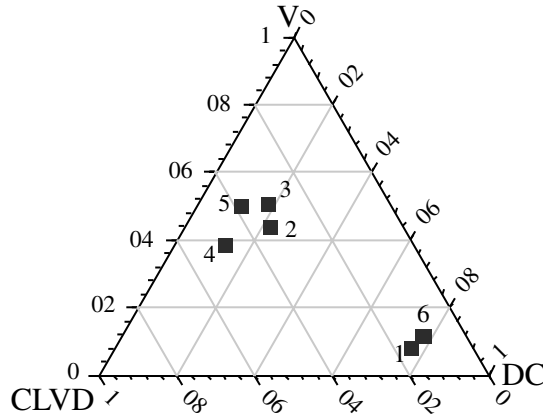
Figure 10
Triangular representation of the moment tensor components for the earthquakes numbered as in Table 5.

high seismicity periods are characterised by energy rates with a clearly increasing trend in time. The first period of increased seismicity is observed around 1977–1980. The average rate of energy release in such a period increases to a value of about 0.3×10^{10} J/month, with respect to the background level which is below 0.1×10^{10} J/month. The second period of seismic crisis occurs in 1989–1990. The energy release rate in this period is of about 0.8×10^{10} J/month, higher than in 1977–1980. In 1989 the first earthquakes with magnitude above 3 appear in the Vesuvius seismic sequence and some years before the 1989 crisis, around 1986, the b value of the sequence changes significantly, from 1.7–1.8, characteristic of the 1972–1986 period, to a lower value (1.3). Such a b value remains practically constant until the subsequent crisis of 1995–1996, when it further decreases, to 1.0, a value that persists until the end of the available to us observations (October, 2000). The evidence that the b-value can significantly decrease in volcanic areas, as a consequence of the fracture coalescence generating progressively larger faults, is supported by recent studies and laboratory experiments (MEREDITH *et al.* 1990). The observed decrease of b is particularly relevant if we consider the recent results obtained by ESPOSITO *et al.* (2000) who estimated a b value ranging between 0.75 and 1.05 in the seismic crises associated with past Vesuvius eruptions.

The crisis of 1995–1996 is characterised by a larger energy rate, with respect to the 1989–1990 period (about 0.9×10^{10} J/month). The last crisis, spanning the end of 1999-beginning of 2000, is characterised by an even higher energy rate, of about 2.0×10^{10} J/month. The maximum earthquake magnitudes during periods of crisis increase with time, from the values $M_d < 3.0$ of 1977–1978 to $M_d = 3.2$ of 1989–1990, $M_d = 3.4$ in 1996 and $M_d = 3.6$ in October 1999. The change in the maximum magnitude of each active period is consistent with the progressive increase of the b value. Furthermore, the b values, whose rapid changes roughly correspond with

periods of crisis, remain constant after the end of each crisis. This progressive escalation of energy release and of the maximum magnitudes during periods of intense activity indicates that the energy involved in the process increases with time and that some peculiar dynamic processes are superimposed to the constant background. A very important point evidenced in this paper is that the seismic sequence exhibits an internal dynamic, pointing towards progressively higher energy rates, and not a repetitive character as would be expected for a simple background activity. From all the existing literature, based on historical observations of pre-eruptive periods, no clear evidence exists for events with magnitudes larger than 4, except perhaps the earthquake which occurred in 62 A.D., 17 years before the 79 plinian eruption. Moreover, no evidence exists for very intense seismicity before large eruptions, so that the period preceding the next eruption also could be characterized by seismic sequences very similar, in number and magnitude, to those observed during recent periods of crisis. Another key point for the evaluation of the eruptive hazard in this area is the careful estimation of the earthquake source properties necessary to understand the nature of the seismicity during the critical periods. The apparent features of most of the observed earthquakes are those normally associated with volcano-tectonic events. However, the reliable determination of the source moment tensor of the most energetic events ($M_d > 3.0$) evidences the presence, in the seismic source, of strong isotropic components, which in most cases indicates explosion. Such isotropic components are statistically significant, at more than 95% significance level, for most of the analysed events, and are in agreement with the observations of low S/P amplitude ratios, as compared with those theoretically expected from the best double couple mechanisms.

The seismicity of Mt. Vesuvius in the last three decades appears to comprise the superposition of a background level and of sporadic periods of intense activity. The genesis of the largest earthquakes occurring during the intense seismicity episodes is likely to involve internal dynamics, linked perhaps to magma movements or to volatile exolution, as indicated by the strong isotropic components, consistent with explosive processes. The inferred non double-couple components, in fact, indicating explosion, are considerably different from those inferred at Mt. Etna (SARAÒ et al., 2001). Such a difference possibly reflects the different magmatic properties of the two areas. At Mt. Etna, where magmas are deficient in volatiles, non double-couple components basically indicate CLVD, i.e., a kind of compensated tensile cracks. At Mt. Vesuvius, where magmas are rich in volatiles generating explosive mixtures, the largest earthquakes are characterised by relevant explosive components in the moment tensor.

In conclusion, even if the common background seismic activity at Somma-Vesuvius, volcano-tectonic in character, does not generate particular concern, sporadic high seismicity episodes must be accurately monitored and evaluated. At the moment, it is not yet possible to uniquely interpret such episodes, nonetheless they

may indicate the presence of an ongoing internal volcanic activity, superimposed to that one generating the ordinary background seismicity.

Acknowledgements

References

Berrino, G., Coppa, U., De Natale, G., and Pingue, F. (1993), *Recent geophysical investigation at Somma-Vesuvio volcanic complex*. In *Mount Vesuvius* (De Vivo B., Scandone R., and Trigila R., editors), J. Volcanology and Geothermal Research *58*, 239–262.

Bianco, F., Castellano, M., Del Pezzo, E., and Ibanez, J. M. (1999), *Attenuation of Short-period Seismic Waves at Mt. Vesuvius, Italy*, Geophys. J. Int. *138*, 67–76.

Brune, J. N. (1970), *Tectonic Stress and the Spectra of Seismic Shear Waves from Earthquakes*, J. Geophys. Res. *75*, 4997–5009.

Campus, P., Cespuglio, G., and Panza, G. F. (1993), *Atti dell'Accademia dei Lincei relativi a International Conference Large explosive eruptions (The Problem of Eruptions, Forecasting Full Moment Tensor Retrieval and Fluid Dynamics in Volcanic Areas: The Case of Plegrean Fields (South Italy), and Warning; Limits and Possibilities)*, 81–101.

Capuano, P., Coppa, U., De Natale, G., Di Sena, F., Godano, C., and Troise, C. (1999), *A detailed analysis of some local earthquakes at Somma-Vesuvius*. In *Physics of volcanic phenomena and eruption precursors* (De Natale G., Gasparini P., Coppa U., editors), Annali di Geofisica *42* (3), 391–405.

Cespuglio, G., Campus, P., and Sileny, J. (1996), *Seismic Moment Tensor Resolution by Waveform Inversion of a Few Local Noisy Records-II. Application to Phlaegrean Fields (Southern Italy) Volcanic Tremors*, Geophys. J. Int. *126*, 620–634.

Del Pezzo, E., Iannaccone, G., Matini, M., and Scarpa, R. (1983), *The 23 November 1980 Southern Italy earthquake*, Bull. Seismol. Soc. Am. *1*, 187–200.

De Natale, G., Capuano, P., Troise, C., and Zollo, A. (1998), *Seismicity at Somma-Vesuvius and its Implication for the 3-D Tomography of the Volcano*, J. Volcanol. Geotherm. Res. *82*, 175–197.

De Natale, G., Petrazzuoli, S. M., Troise, C., Pingue, F., and Capuano, P. (2000), *Internal Stress at Mt. Vesuvius: A Model for Background Seismicity at Central Volcano*, Geophys. Res. *105* (B7), 16,207–16,214.

Esposito, E., Mastrolorenzo, G., and Porfido, S. (2000), *Seismicity at Vesuvius, a Comparison between Historical Eruptive Periods and Present Time*. Abstract. EGS 2000. Nizza, France.

Florsch, N., Fäh, D., Suhadolc, P., and Panza, G. F. (1991), *Complete Synthetic Seismograms for High-Frequency Multimode SH-waves*, Pure Appl. Geophys. *136*, 529–560.

Gutenberg, B. and Richter, C. F. (1944), *Frequency of Earthquakes in California*, Bull. Seismol. Soc. Am. *34*, 185–188.

Gutenberg, B. and Richter, C. F. (1956), *The energy of earthquakes*. Q. J. Geol. Soc. London, *112*, 1–14.

Iannaccone, G., Alessio, G., Borriello, G., Cusano, P., Petrosino, S., Ricciolino, P., Talarico, G., and Torello, V. (2001), *Characteristics of the Seismicity of Vesuvius and Campi Flegrei during the year 2000*, Annali di Geofisica *44* (5/6), 1075–1091.

JOST, M. L. and HERRMANN, R. B. (1989), *A Student's Guide to and Review of Moment Tensors*, Seismol. Res. Lett. *60*, 37–57.

KANAMORI, H., MORI, J., HAUKSSON, E., HEATON, TH., HUTTON, L. K., and JONES, L. M. (1993), *Determination of Earthquake Energy Release and ML Using TERRASCOPE*, Bull. Seismol. Soc. Am. *83*, 2, 330–346.

KNOPOFF, L. and RANDALL M. (1970), *The Compensated Linear-vector Dipole: A Possible Mechanism for Deep Earthquakes*, J. Geophys. Res. *75*, 4957–4963.

KRAVANJA, S., PANZA, G. F., and SILENY, J. (1999), *Robust Retrieval of a Seismic Point-source Time Function*, Geophys. J. Int. *136*, 385–394.

MARTURANO, A. and RINALDIS, V. (1995), *Archeaologie und Seismology* (Verlag Biering and Brinkmann, München) pp. 131–135.

MARTURANO, A. and RINALDIS, V. (1996), *Seismic History and Consistent Seismicity; Evidence from Southern Italy*, Natural Hazards *14*, 11–21.

MARZOCCHI, W., VILARDO, G., HILL, D. P., RICCIARDI, G. P., and RICCO, C. (2001), *Common Features and Peculiarities of the Seismic Activity at Phlegraean Fields, Long Valley, and Vesuvius.* Bull. Seismol. Soc. Am. *91*, 191–205.

MEREDITH, P. G., MAIN, I. G. and JONES C. (1990), *Temporal variations in seismicity during quasi-static and dynamic rock failure*, Tectonophysics, *175*, 249–268.

MOLCHAN, G. M. and PODGAETSKAYA, V. M. (1973), *Parameters of global seismicity*. In (*V. I. Keilis-Borok, ed.*), *Comput. Seismology*; *6*, Nauka, Moscow, 44–66 (in Russian).

MOLCHAN, G., KRONROD, T., and PANZA, G. F. (1997), *Multi-scale Seismicity Model for Seismic Risk*, Bull. Seismol. Soc. Am. *87*, 1220–1229.

NABELEK, J. L. (1984), *Determination of Earthquake Source Parameters from Inversion of Body Waves*, Ph.D. Thesis, Massachusetts Institute of Technology, Cambridge, USA.

PANZA, G. F. (1985), *Synthetic Seismograms: The Rayleigh Waves Modal Summation*, J. Geophys. *58*, 125–145.

PANZA, G. F. and PROZOROV, A. (1991), *High Frequency Seismic Sources Characterize the Areas of Tectonic Shortening in the Italian Region*, Rend. Fis. Acc. Lincei *2*, 107–116.

PANZA, G. F. and SARAÒ, A. (2000), *Monitoring Volcanic and Geothermal Areas by Full Seismic Moment Tensor Inversion: Are Non-double Couple Components Always Artefacts of Modeling?* Geophys. J. Int. *143*, 353–364.

PANZA, G. F., ROMANELLI, F., and VACCARI, F. (2001), *Seismic Wave Propagation in Laterally Heterogeneous Anelastic Media: Theory and Applications to Seismic Zonation*, Advances in Geophysics *43*, 1–95.

RIEDESEL, M. A. and JORDAN, T. H. (1989), *Display and Assessment of Seismic Moment Tensors*, Bull. Seismol. Soc. Am. *79*, 85–100.

ROLANDI, G., BARRELLA, A. M., and BORRELLI, A. (1993), *The 1631 Eruption of Vesuvius*, Volcanol. Geotherm. Res. *58*, 183–201.

ROSI, M., PRINCIPE, C., and VECCI, R. (1993), *The 1631 Vesuvius Eruption. A Reconstruction Based on Historical and Stratigraphical Data*, J. Volcanol. Geotherm. Res. *58*, 151–182.

SANTACROCE, R. (ed.), (1987), *Somma-Vesuvius*. Quaderni dell Ricerca Scientifica, CNR Roma *114*, 1–251.

SARAÒ A., PANZA, G. F., PRIVITERA, E., and COCINA, O. (2001), *Non-double Couple Mechanisms in the Seismicity Preceeding 1991–1993 Etna Volcano Eruption*, Geophys. J. Int. *145*, 319–335.

SCANDONE, R., GIACOMELLI, L., and GASPARINI (1993), *Mount Vesuvius: 2000 Years of Volcanological Observations*, J. Volcanol. Geotherm. Res. *58*, 5–25.

SIGURDSSON, H., CAREY, S., CORNELL, W., and PESCATORE, T. (1985), *The Eruption of Vesuvius on AD 79*, Natl. Geogr. Res. *1*, 332–387.

SILENY, J., PANZA, G. F., and CAMPUS, P. (1992), *Waveform Inversion for Point Source Moment Tensor Retrieval with Optimization of Hypocentral Depth and Structural Model*, Geophys. J. Int. *108*, 259–274.

SILENY, J., CAMPUS, P., and PANZA, G. F. (1996), *Seismic Moment Tensor Resolution by Waveform Inversion of a Few Local Noisy Records—I. Synthetic Tests.* Geophys. J. Int. *126*, 605–619.

SILENY, J. (1998), *Earthquake Source Parameters and their Confidence Regions by a Genetic Algorithm with a "Memory"*, Geophys. J. Int. *134*, 228–242.

SILENY, J. and VAVRYCUK, V. (2000), *Approximate Retrieval of the Point Source in Anisotropic Media: Numerical Modelling by Indirect Parameterization of the Source*, Geophys. J. Int. *143* (3), 700–708.

SIPKIN, S. A. (1982), *Estimation of Earthquake Source Parameters by the Inversion of Waveform Data: Synthetic Waveforms*, Phys. Earth. Planet. Inter. *30*, 242–259.

STUMP, B. V. and JOHNSON, L. R. (1977), *The Determination of Source Properties by the Linear Inversion of Seismograms*, Bull. Seismol. Soc. Am. *67*, 1489–1502.

VILARDO, G. (1996), *Rapporto sismico Vesuviano del 25 April 1996*, Report Osservatorio Vesuviano, Napoli.

VILARDO, G., VENTURA, G., and MILANO, G. (1999), *Factors Controlling the Seismicity of the Somma-Vesuvius Volcanic Complex*, Volcanology and Seismology *20* (2) 219–238.

VILARDO, G., BIANCO, F., CAPELLO, M., CASTELLANO, M., and MILANO, G. (2002), *Mt Vesuvius Seismic Activity*, *1996*. Acta Vulcanologica, in press.

WIEMER, S. and ZUNIGA, R. F. (1994), *ZMAP – A Software Package to Analyze Seismicity*, EOS, Transactions, Fall Meeting, AGU *75*, 456.

ZOLLO, A., GASPARINI, P., VIRIEUX, J., LE MEUR, H., DE NATALE, G., BIELLA, G., BOSCHI, E., CAPUANO, P., DE FRANCO, R., DELL'AVERSANA, P., DE MATTEIS, R., GUERRA, I., IANNACCONE, G., MIRABILE, L., and VILARDO, G. (1996), *Seismic Evidence for a Low-Velocity Zone in the Upper Crust Beneath Mount Vesuvius*, Science *274* (5287), 592–594.

To access this journal online:
http://www.birkhauser.ch